Optically Active Chiral CuO 'Nanoflowers'

ARTICLE *in* JOURNAL OF THE AMERICAN CHEMICAL SOCIETY · MAY 2014

Impact Factor: 12.11 · DOI: 10.1021/ja500197e · Source: PubMed

JACS
JOURNAL OF THE AMERICAN CHEMICAL SOCIETY
Communication
pubs.acs.org/JACS

Optically Active Chiral CuO "Nanoflowers"

Yingying Duan,[†,§] Xiao Liu,[†,§] Lu Han,[†,§] Shunsuke Asahina,[‡] Dongdong Xu,[†] Yuanyuan Cao,[†] Yuan Yao,[†] and Shunai Che*[,†]

[†]School of Chemistry and Chemical Engineering, State Key Laboratory of Metal Matrix Composites, Shanghai Jiao Tong University, 800 Dongchuan Road, Shanghai, 200240, P. R. China

[‡]SMBU, JEOL, Akishima Tokyo 196-8558, Japan

Supporting Information

ABSTRACT: Helical symmetry can be found in most flowers with a rotation of contort petal aestivation. For micro- and nanoscale analogies, flower mimicking structures have been reproduced; however, the conceptual chirality of "nanoflowers" has not yet been defined. Here, the chirality of the "flower" was defined by its nanosized chiral structure and consequent optical activity (OA), opening new horizons for the physical theory and chiral materials. We report the surfactant-mediated hydrothermal synthesis of chiral CuO nanoflowers using sodium dodecyl sulfate (SDS) as a structure-directing agent, an amino alcohol as a symmetry-breaking agent, and cupric salt as the inorganic source. Two levels of hierarchical chirality exist for a CuO nanoflower including primary helically arranged "nanoflakes" and secondary helical "subnanopetals" that form "nanopetals". The nanoflowers exhibited a prominent optical response to circularly polarized light (CPL) at the absorption bands characteristic of CuO.

Although the chiral structures of most open flowers are less prominent, the flowers are considered intrinsically chiral because their origins are always pronounced in floral buds.[1,2] The chirality in asymmetric floral structures is often defined via macroscopic observation.[1,2] Various macroscopic flowers such as peony-, chrysanthemum-, rose-, and dandelion-like flowers with nanorod, nanosheet, nanoflake, and nanoplate petals were successfully synthesized via microwave heating or a hydrothermal reflux method based on the self-assembly of simple amphiphiles and peptides with various inorganic sources onto inorganic materials (e.g., semiconductors, metal oxides, carbonates, and phosphates)[3−9] and pure organic materials (e.g., polymer and DNA aggregations).[10,11] Because chirality begets handedness and handedness begets optical activity (OA), the OA of the nanoflowers can define their chirality.[12−19] Although these nanoflowers are actually chiral, these materials do not result in OA, and researchers are not interested in their chirality, probably because either racemic flowers form in the presence of achiral organics or unit petals form that are too large even in the chiral molecules of the structure-directing systems.

In this investigation, the sodium dodecyl sulfate (SDS) surfactant was chosen as a structure-directing agent for the cupric ions due to its high amphiphilicity in aqueous solution and the electrostatic interaction between the negatively charged sulfate headgroup and the positively charged cupric ions, which play a significant role in regulating the CuO nanoparticle morphology.[20] From the enormous chiral molecules, antipodal (*S*)-(−)- and (*R*)-(+)-2-amino-3-phenyl-1-propanol ((*S*)-(−)- and (*R*)-(+)-APP) were chosen as symmetry-breaking agents due to the co-operative assembly effect from their amino alcohol groups chelating well with the cupric ions and benzene ring interacting with the hydrophobic tail of the SDS. The cupric ions serve as an inorganic source and bridge due to the dual interactions with the negatively charged sulfate SDS headgroup and the coordination bonding chelation with the amino alcohol groups of the APP. The copper oxide crystals with a chiral architecture can be formed through the cooperative interaction between the structure-directing agent, the symmetry-breaking agent, and the inorganic source. When the organics are removed via washing, pure chiral CuO in its tenorite form can be obtained. This material exhibits characteristic absorption bands in the UV−visible region due to various monoclinic CuO transitions (space group $C2/c$) and induces an electron transition-based OA (ETOA) under a dissymmetric electric field.[19,21]

Figure 1 provides scanning electron microscopy (SEM) and high-resolution transmission electron microscopy (HRTEM) images of the samples synthesized using (*S*)-(−)-APP for 75 and 135 min (see also Figure S1 for purity), respectively. The samples were composed of uniform flower-like particles with diameters that range from 1.0 to 2.5 μm (Figure S1). Figure 1a$_1$ and b$_1$ indicate that the well-defined peony-like CuO nanoflowers present three-dimensional (3D) microstructures assembled with many densely and randomly arranged nanopetals grown from the center of the flower. The chiral arrangement of these nanopetals is not obvious in the open flower forms, but the flower may be intrinsically chiral because of its chiral origin.[2] As shown in Figure 1a$_2$ and b$_2$, these nanopetals are composed of several subnanopetals with widths ranging from 50 to 100 nm. The subnanopetals are stacked in a single direction and are alternately connected, which clearly reveals the handedness of the helical structure. When extending the reaction time, the "flowers" became denser and smoother, the "petals" thickened, and their chiral arrangement became clearer. The flower-like CuO nanoparticles formed with the (*R*)-(+)-APP exhibited the same structure in the opposite direction (Figure S2). Consequently, antipodal chiral CuO

Received: January 9, 2014
Published: May 6, 2014

dx.doi.org/10.1021/ja500197e | *J. Am. Chem. Soc.* 2014, 136, 7193−7196

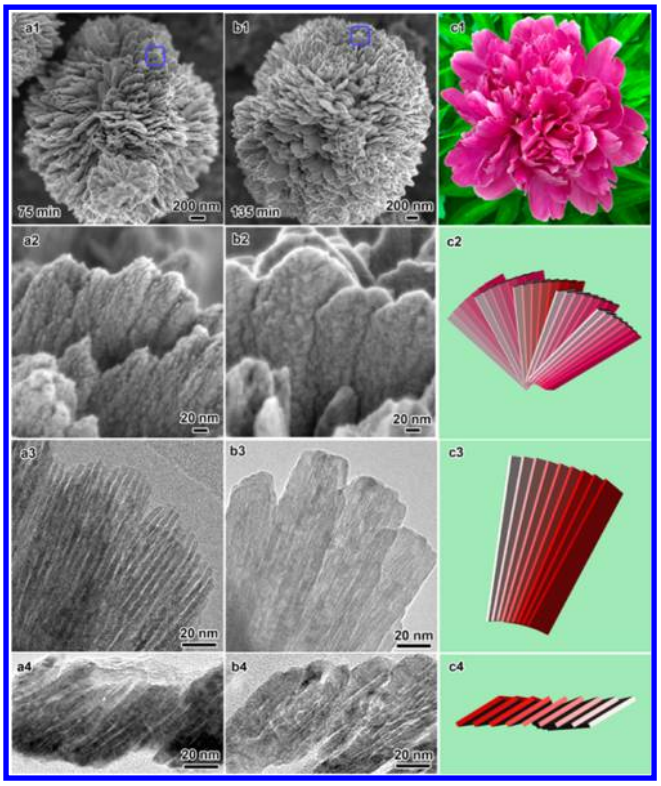

Figure 1. SEM and HRTEM images of varying magnification and schematic drawings of sinistrorse CuO nanoflowers (S-CuO) synthesized with (*S*)-(−)-APP at synthesis times of 75 min (a) and 135 min (b). (a_1−c_1) Peony-like CuO nanoflowers with randomly stacked nanopetals. (a_2−c_2) Nanopetals with helically arranged subnanopetals. (a_3−c_3) Fan-shaped assembly of nanoflakes in subnanopetals. (a_4−c_4) Cross section of the helically arranged nanoflakes. The synthetic molar composition was 1.0 SDS/1.0 (*S*)-(−)-APP/60 NaOH/1.0 Cu^{2+}/2000 H_2O.

nanoflowers with subnanopetals of the opposite handedness were synthesized in the presence of antipodal APP molecules. The nanoflowers with subnanopetals arranged in a counterclockwise manner are defined as sinistrorse (or left-handed) (Figure $1c_2$), and those with a clockwise arrangement are defined as dextrorse (or right-handed) (Figure S2c3). The sinistrorse and dextrorse CuO nanoflowers are denoted as S-CuO or D-CuO, which were formed with (*S*)-(−)- and (*R*)-(+)-APP, respectively.

As depicted in Figure $1a_{2-3}$ and b_{2-3}, SEM and HRTEM images show that each subnanopetal in the nanoflowers consists of a dozen anisotropic nanoflakes growing from the center of the flower. The TEM images of its cross section (Figure $1a_4$ and $1b_4$) indicate that the nanoflake arrangements are exclusively left-handed for S-CuO (inclination angle below 90°) and right-handed for D-CuO (inclination angle above 90° as demonstrated in Figure $S2a_5$ and $S2b_5$). These cases of handedness are consistent with those of the subnanopetals. When extending the synthesis time from 75 to 135 min, the nanoflake thickness and width increased from ∼4 to ∼6 nm and from ∼60 to ∼90 nm, respectively, to form thick subpetals and thus thick petals. Similar CuO nanoflowers have been achieved using other amino alcohol chiral molecules that can strongly chelate with cupric ions and either inorganic or organic cupric salts (not shown).

The wide-angle powder X-ray diffraction (PXRD) patterns of the antipodal chiral CuO nanoflowers of varying reaction times (Figures 2 and S3) present identical reflections indexed as the monoclinic crystal structure of CuO with a space group of *C*2/*c*

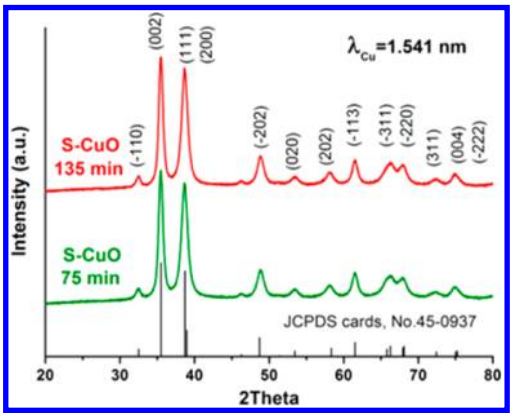

Figure 2. XRD patterns of the S-CuO nanoflowers depicted in Figure 1.

[JCPDS cards, No. 45-0937]. The reflections of the sample synthesized over 135 min are higher and narrower than those over 75 min, indicating that the crystallinity and particle size of the samples increase, which is consistent with the SEM and TEM observation. Additionally, the absence of organics in the as-prepared sample has been confirmed via Fourier transform infrared (FTIR) spectroscopy (Figure S4), elemental analysis (Table S1), and solid-state ^{13}C CP/MAS NMR (Figure S5), which indicate that the structure-directing agent, SDS, and the chiral symmetry-breaking agent, APP, can be easily removed by washing.

The fine crystalline structure of the nanoflakes was observed via HRTEM as presented in Figure 3. The well-resolved lattice fringes of the monoclinic CuO and corresponding Fourier diffractograms (FDs) indicate that each nanoflake is a single crystal and that all nanoflakes of the subnanopetals exhibit the same orientation aligned along the [011] zone axis, but with a rotational relationship along a tiny angle. The angle of the seven flakes shown in Figure $3a_1$ changed gradually from −5.1° to +9.1° relative to the central flake (red in Figure $3a_1$) from left to right, indicating a fan-shaped arrangement of the nanoflakes overlapping in the center of the flowers and simultaneously rotated clockwise or counterclockwise, as shown in Figure $1c_3$. The {1−11} facets of the nanoflakes were exposed as a dominant facet and the crystal stacked layer-by-layer on the {1−11} to form the subnanopetals, as indicated by the model in Figure $3a_2$−h_2.[22] From the cross-sectional HRTEM images (Figure S6), the exposed facets of the flakes can be confirmed as {1−11}.

The OA is known to be the primary attribute of molecular and microscopic chiral materials. Therefore, the chiral stacking of CuO nanoparticles should endow the CuO nanoflowers with OA, which can be easily detected via diffused reflection circular dichroism (DRCD). Figure 4a presents the DRCD and diffused reflection ultraviolet−visible (DRUV−vis) spectra of the antipodal CuO nanoflower pairs with temperature-maintained durations of 75 and 135 min.

The UV−vis spectra of the nanoflowers exhibited a broad absorption band across the entire wavelength range, which was attributed to the overlap of various CuO characteristic absorption bands.[21] The absorption in the 250−280 nm range could correspond to the $O^{2-}(2p) \rightarrow Cu^{2+}(3d)$ ligand-to-metal charge transfer transition; the bands at 320−440 nm

dx.doi.org/10.1021/ja500197e | *J. Am. Chem. Soc.* 2014, 136, 7193−7196

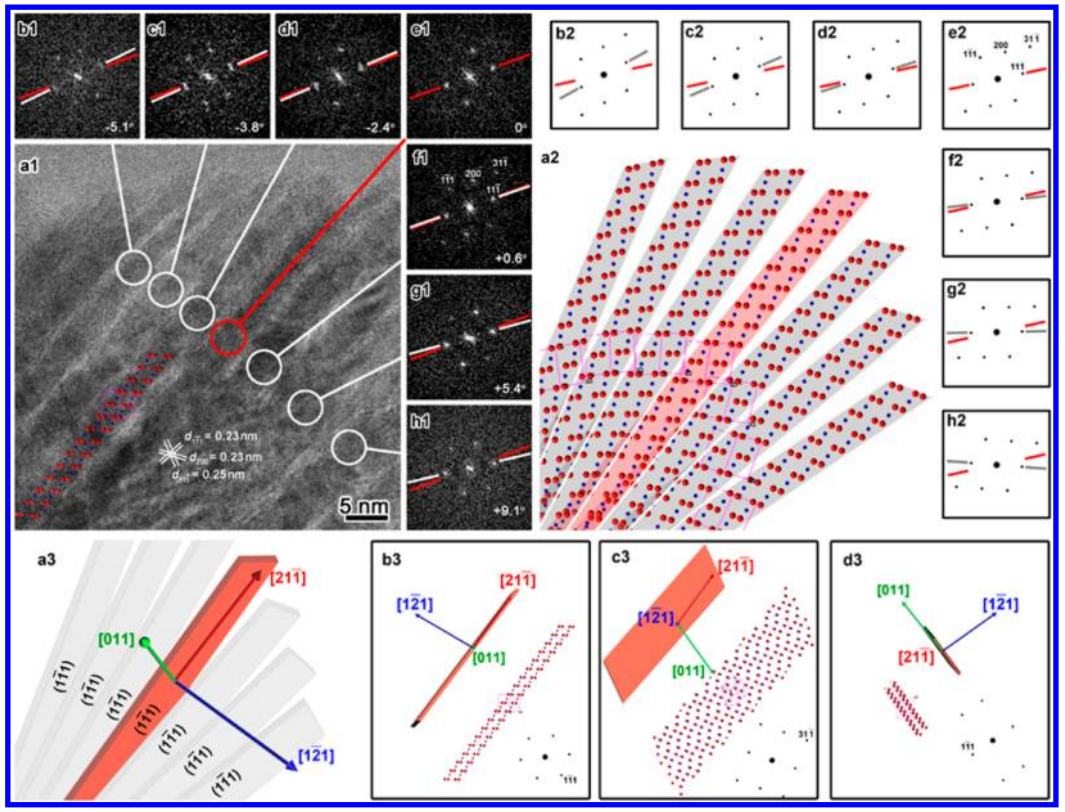

Figure 3. (a_1–h_1) HRTEM image and the corresponding FDs of the nanoflake taken with the [011] indices of the CuO exhibiting the single crystallinity of each flake with exposed {1−11} facets and a fan-shaped arrangement. (a_2–h_2) The structural model of the CuO crystal nanoflakes with a fan-shaped arrangement. (a_3–d_3) The crystal structure of the CuO nanoflake illustrates the relationship between the growing direction of the flake and the unit cell of the monoclinic CuO crystal. The light red rectangle denotes a rectangular flake.

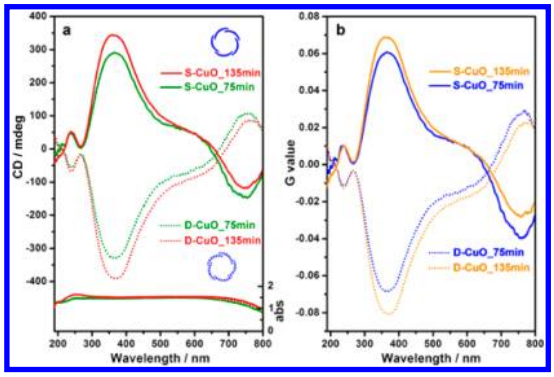

Figure 4. DRUV−vis absorption and DRCD spectra (a) and the Kuhn anisotropy g value (b) of the antipodal (S- and D-CuO) chiral CuO nanoflowers presented in Figures 1 and S2 indicate that the UV absorption and experimental mirror-image CD signals occurred at the CuO absorption band, confirming that the nanoflower OA arises from the chiral structure of the CuO.

would indicate the charge transfer transition of Cu^{2+}−O^{2-}−Cu^{2+}; and the peaks at 600−700 nm could be assigned to the d−d transitions of Cu^{2+} with various symmetries.

Experimental mirror-imaged CD spectra were obtained for these CuO products and indicated that chiral nonracemic CuO were produced. The CD spectra of the antipodal samples exhibit a weak peak at ∼240 nm, a strong peak at ∼360 nm, and shoulders at ∼550 and ∼750 nm, corresponding to the aforementioned three absorption bands of the CuO crystals and Cu^{2+} and not to the chiral organic symmetry breaking agent (Figure S7). The Kuhn anisotropy factor $g_\lambda = \Delta\varepsilon/\varepsilon = 2(\varepsilon_L - \varepsilon_R)/(\varepsilon_L + \varepsilon_R)$ are also plotted in Figure 4b for as-synthesized CuO nanoflower samples. The maximum value found is as large as $|g_{360}| = 0.08$. The CD signals can be attributed to the helical stacking of the CuO nanoparticles in close proximity.[23,24] The helically aggregated nanoflakes and subnanopetals comprise a single "chromophore entity" with different levels via a series of collective excitation modes that can be delocalized to dimensions comparable to that of the entire aggregate. Hence, we believed that the Cotton effects centered at ∼240 and ∼750 nm could be recognized as the excitation coupling of the $O^{2-} \rightarrow Cu^{2+}$ charge transfer transition and the d−d transitions of Cu^{2+} under a dissymmetric electron field, respectively, for which a slight blue shift also indicated the influence of the quantum size effect.[25] These overlapped signals represent the hierarchical chirality, i.e., the excitation coupling between the nanoflakes and subnanopetals. The CD signal intensity increased with increasing reaction time due to the increasing density of the "flakes" in the thick "petals". After calcination in air at 550 °C, nanoflakes were no longer observable in either the SEM or TEM images; however, the CD signals maintained their shapes and intensity, indicating that the two levels of chirality were perfectly maintained but that the flakes in close proximity formed thick petals (Figure S8). One may believe that the CD signals may be due to surface imprinting, in which the chiral structure directing agent leaves a chiral structure of the CuO on its surface,[26−29] or due to the chiral arrangement of Cu atoms.[30,31] CD signals originating from the chiral surface arrangements at atomic scale would be superimposed with the CD bands attributable to the helical geometry at nanoscale. However, our experimental data of the

dx.doi.org/10.1021/ja500197e | J. Am. Chem. Soc. 2014, 136, 7193−7196

man-made destroying flowers process (Figure S9), scrutiny of the synthesis parameters for the CuO nanoflower (Figure S10–S12), synthesis of CuO with different (*S*)-(−)/(*R*)-(+)-APP molar ratios (Figure S13), dispersion of commercial CuO powder in the (*S*)-(−)-APP solution (Figure S14), and the real-time tracking experiment of the formation process (see Supporting Information) exhibit that the CD signals disappeared with the absence of the chiral arrangement of nanounits, indicating the OA of the CuO nanoflower arises from the helical arrangement of nanounits rather than surface imprinting.[32]

Consequently, the inorganic flower with electron transition based OA was first synthesized via the self-assembly of an amphiphilic molecule, a symmetry-breaking chiral molecule, and an inorganic source. The chirality of the flower has been defined through a hierarchical nanosized chiral structure and has a strong response to the CPL over a large range of wavelengths of light. Our results provide new conceptual insights into the relationship between optically active materials and natural asymmetric structures and morphologies regarding the functional metamaterials and the physical theory behind electromagnetic wave–chiral structure interactions. The hydrothermal synthesis of such nature mimicked chiral materials would enable hierarchical structures in size and in morphology with electronic level OA over a broad range of wavelengths in the electromagnetic wave spectrum. Therefore, (i) the electronic asymmetries can arise through the manipulation of relative quantum phases in molecular systems and may induce molecular asymmetries of other related molecules, which would open up a new chiral physics and chemistry research area; (ii) a hierarchical chirality constructed with different helices from primary to hierarchical levels, e.g. films with the chiral flowers and spanning a large range of wavelengths, would make their application widespread, such as in electronics, photonics, photocatalysts, biosensors, etc.[15,33−35]

■ ASSOCIATED CONTENT

Supporting Information

Materials and detailed experimental procedures, supplementary table and figures, and results of real-time tracking experiments. This material is available free of charge via the Internet at http://pubs.acs.org.

■ AUTHOR INFORMATION

Corresponding Author

chesa@sjtu.edu.cn

Author Contributions

[§]Y.D., X.L., and L.H. contributed equally to this work.

Notes

The authors declare no competing financial interest.

■ ACKNOWLEDGMENTS

This work was supported by the National Basic Research Program (2013CB934101) and the National Natural Science Foundation (Grant No. 21201120) of China and Evonik Industries. We thank the Instrumental Analysis Centre of Shanghai Jiao Tong University for their collaboration on the DRCD measurements.

■ REFERENCES

(1) Thitamadee, S.; Tuchihara, K.; Hashimoto, T. *Nature* **2002**, *417*, 193.
(2) Endress, P. K. *Curr. Opin. Plant Biol.* **2001**, *4*, 86.
(3) Noorduin, W. L.; Grinthal, A.; Mahadevan, L.; Aizenberg, J. *Science* **2013**, *340*, 832.
(4) Erb, R. M.; Son, H. S.; Samanta, B.; Rotello, V. M.; Yellen, B. B. *Nature* **2009**, *457*, 999.
(5) Ge, J.; Lei, J.; Zare, R. N. *Nat. Nanotechnol.* **2012**, *7*, 428.
(6) Shen, X. F.; Yan, X. P. *Angew. Chem., Int. Ed.* **2007**, *46*, 7659.
(7) King'ondu, C. K.; Iyer, A.; Njagi, E. C.; Opembe, N.; Genuino, H.; Huang, H.; Ristau, R. A.; Suib, S. L. *J. Am. Chem. Soc.* **2011**, *133*, 4186.
(8) Xiong, S.; Chen, J. S.; Lou, X. W.; Zeng, H. C. *Adv. Funct. Mater.* **2012**, *22*, 861.
(9) Nakanishi, T.; Ariga, K.; Michinobu, T.; Yoshida, K.; Takahashi, H.; Teranishi, T.; Möhwald, H.; Kurth, D. G. *Small* **2007**, *3*, 2019.
(10) Hu, J.; Liu, G.; Nijkang, G. *J. Am. Chem. Soc.* **2008**, *130*, 3236.
(11) Zhu, G.; Hu, R.; Zhao, Z.; Chen, Z.; Zhang, X.; Tan, W. *J. Am. Chem. Soc.* **2013**, *135*, 16438.
(12) Berova, N.; Nakanishi, K.; Woody, R. W. *Circular dichroism: principles and applications*, 2nd ed.; Wiley-VCH: New York, 2000.
(13) Barron, L. D. *Molecular light scattering and optical activity*; Cambridge University Press: New York, 2004.
(14) Bartus, J.; Weng, D.; Vogl, O. *Monatsh. Chem.* **1994**, *125*, 671.
(15) Robbie, K.; Broer, D. J.; Brett, M. J. *Nature* **1999**, *399*, 764.
(16) Chen, W.; Bian, A.; Agarwal, A.; Liu, L.; Shen, H.; Wang, L.; Xu, C.; Kotov, N. A. *Nano Lett.* **2009**, *9*, 2153.
(17) Shopsowitz, K. E.; Qi, H.; Hamad, W. Y.; MacLachlan, M. J. *Nature* **2010**, *468*, 422.
(18) Kuzyk, A.; Schreiber, R.; Fan, Z.; Pardatscher, G.; Roller, E.-M.; Högele, A.; Simmel, F. C.; Govorov, A. O.; Liedl, T. *Nature* **2012**, *483*, 311.
(19) Liu, S.; Han, L.; Duan, Y.; Asahina, S.; Terasaki, O.; Cao, Y.; Liu, B.; Ma, L.; Zhang, J.; Che, S. *Nat. Commun.* **2012**, *3*, No. 1215.
(20) Reddy, S.; Kumara Swamy, B. E.; Jayadevappa, H. *Electrochim. Acta* **2012**, *61*, 78.
(21) Praliaud, H.; Mikhailenko, S.; Chajar, Z.; Primet, M. *Appl. Catal. B: Environ.* **1998**, *16*, 359.
(22) Sun, S.; Sun, Y.; Zhang, X.; Zhang, H.; Song, X.; Yang, Z. *CrystEngComm* **2013**, *15*, 5275.
(23) Keller, D.; Bustamante, C. *J. Chem. Phys.* **1986**, *84*, 2972.
(24) Dick, B. *ChemPhysChem* **2011**, *12*, 1578.
(25) Brus, L. E. *J. Chem. Phys.* **1984**, *80*, 4403.
(26) Lahav, M.; Kharitonov, A. B.; Willner, I. *Chem.—Eur. J.* **2001**, *7*, 3992.
(27) Duran Pachon, L.; Yosef, I.; Markus, T. Z.; Naaman, R.; Avnir, D.; Rothenberg, G. *Nat. Chem.* **2009**, *1*, 160.
(28) Lacasta, S.; Sebastián, V.; Casado, C.; Mayoral, A.; Romero, P.; Larrea, A.; Vispe, E.; López-Ram-de-Viu, P.; Uriel, S.; Coronas, J. *Chem. Mater.* **2011**, *23*, 1280.
(29) Zhou, Y.; Yang, M.; Sun, K.; Tang, Z.; Kotov, N. A. *J. Am. Chem. Soc.* **2010**, *132*, 6006.
(30) Switzer, J. A.; Kothari, H. M.; Poizot, P.; Nakanishi, S.; Bohannan, E. W. *Nature* **2003**, *425*, 490.
(31) Widmer, R.; Haug, F. J.; Ruffieux, P.; Gröning, O.; Bielmann, M.; Gröning, P.; Fasel, R. *J. Am. Chem. Soc.* **2006**, *128*, 14103.
(32) Ma, W.; Kuang, H.; Wang, L.; Xu, L.; Chang, W.-S.; Zhang, H.; Sun, M.; Zhu, Y.; Zhao, Y.; Liu, L.; Xu, C.; Link, S.; Kotov, N. A. *Sci. Rep.* **2013**, *3*, No. 1934.
(33) Broer, D. J.; Lub, J.; Mol, G. N. *Nature* **1995**, *378*, 467.
(34) Gansel, J. K.; Thiel, M.; Rill, M. S.; Decker, M.; Bade, K.; Saile, V.; von Freymann, G.; Linden, S.; Wegener, M. *Science* **2009**, *325*, 1513.
(35) Bao, Q.; Zhang, H.; Wang, B.; Ni, Z.; Lim, C. H. Y. X.; Wang, Y.; Tang, D. Y.; Loh, K. P. *Nat. Photonics* **2011**, *5*, 411.